

DETERMINING ORBITAL PARTICLE PARAMETERS OF IMPACTS INTO GERMANIUM
USING MORPHOLOGY ANALYSIS AND CALIBRATION DATA FROM HYPERVELOCITY
IMPACT EXPERIMENTS IN THE LABORATORY

Klaus G. Paul*

Lehrstuhl für Raumfahrttechnik, TU München
Richard-Wagner-Straße 18/III
D-80333 München, Germany
Phone: (+) 49 89 2105 2578, Fax: (+) 49 89 2105 2468
E-Mail: kpaul@asterix.lrt.mw.tu-muenchen.de

545-39
113 935
108

SUMMARY

This paper describes the work that is done at the Lehrstuhl für Raumfahrttechnik (Lrt) at the Technische Universität München to examine particle impacts into germanium surfaces which were flown on board the LDEF satellite. Besides the description of the processing of the samples, a brief overview of the particle launchers at our institute is given together with descriptions of impact morphology of high- and hypervelocity particles into germanium. Since germanium is a brittle, almost glass-like material, the impact morphology may also be interesting for anyone dealing with materials such as optics and solar cells.

The main focus of our investigations is to learn about the impacting particle's properties, for example mass, velocity and direction. This is done by examining the morphology, various geometry parameters, crater obliqueness and crater volume.

LDEF EXPERIMENT A0187-2

Experiment Description

The Experiment "Chemical and Isotopical Measurements of Micrometeoroids using SIMS" has been described elsewhere in greater detail ([2] and [11]). It occupied three locations: one 1/1 tray on bay E08, one 2/3 tray on bay E03, and one 1/3 tray on bay C02. A thin foil covered germanium targets and should cause impacting particles to break up and produce a large amount of residue spray, which we call "extended impacts". See figure 1 for a cross-sectional sketch of the experiment setup.

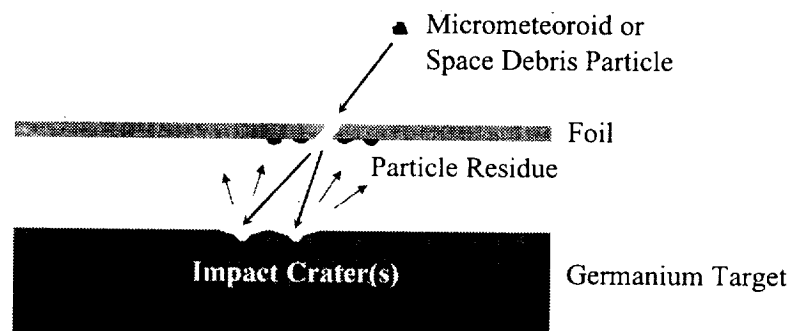


Figure 1. Cross-sectional sketch of capture cell of experiment A0187-2 "Chemical and Isotopical Measurements of Micrometeoroids using Secondary Ion Mass Spectrometry"

After LDEF recovery it turned out that most of the foils were destroyed, thus allowing many impacting particles to produce regular hypervelocity impacts. Only some foils from the trailing edge trays remained intact.

The lrt received nine capture cells from tray E08, each containing four 39x42x0.5 mm germanium wafers, plus two circular impact cells from EEEEC experiment S1002. This paper focuses on the capture cells from tray E08.

LDEF Sample Processing

The LDEF samples were first scanned in order to locate impact features using a Cambridge Stereoscan S120 scanning electron microscope at a magnification of 100x. Once an impact feature was found, it was classified as impact, extended impact or unusual pattern. However, the patterns labeled as unusual seemed to be contamination patterns similar to those found on other surfaces as well as reported by several other investigators. Only the impact features with an obvious spray pattern formed during the impact were regarded as extended impacts.

A total number of 907 impact features (895 conventional impacts and 12 extended impacts) have so far been found on two capture cells, resulting in a total scanned area of $13.1 \cdot 10^{-3} \text{ m}^2$.

Once an impact has been identified its image is stored on a standard, frame-grabber equipped PC. This image is then used to sketch the exact shape of the crater, resulting in grater detail than previous investigations [5], for size and geometry information. The outline image is then converted into an ASCII readable format that can be used for calculating the various crater areas (see figure 2). We distinguish between (a) central crater, (b) secondary spallation zone (i.e. all the visible damaged area) and (c) chips that remained in the impact feature. Radial cracks, visible near some of the impact features, were ignored in the sketches. Up to now, 615 impact features have been sketched.

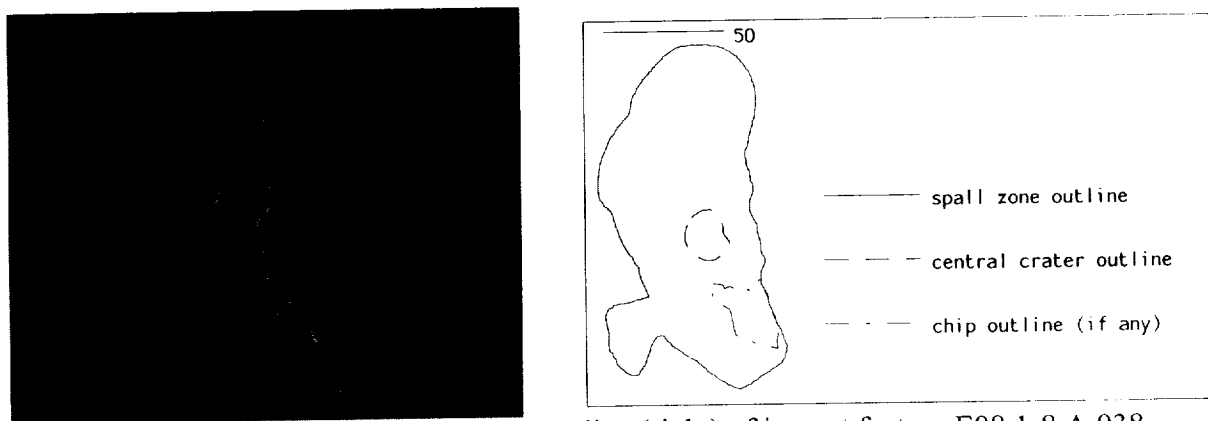


Figure 2. GIF image (left) and redrawn outline (right) of impact feature E08 1-8 A 038

We also take an even closer look at the impact feature geometry. Using a Rodenstock RM600/3-D laser topographer a three-dimensional map of the impact features is created. This instrument typically returns z-coordinates within a range of $\pm 300 \mu\text{m}$ and an accuracy of better than 0.5% with some 400 points per mm along its measurement axis and $2 \mu\text{m}$ offsets between each measurement.

This three-dimensional data allows not only the determination of otherwise almost not measurable properties, such as crater or impact feature volume, but also a close look at crater cross-sections and, therefore, crater depths. See figures 19 and 21 for examples of such a scan, figures 24 through 28 for cross-sectional scans, references [6] and [13] for pictures of actual cross-sections showing hidden caverns under the surface that cannot be measured with our topographer.

Impact Morphology

Basically, we discriminate between two different types of impact features: Extended impacts that show signs of foil interaction, and standard high- and hypervelocity impact features resembling the typical patterns already described for example in [1], [10] and [14]. See figures 3 and 4 for examples of such impact features.



Figure 3. Extended impact feature showing the typical spray pattern of a particle that was broken up

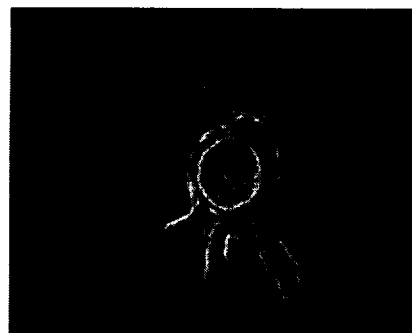


Figure 4. Standard hypervelocity impact with molten central crater and impact residue (molten spheres) around the impact feature



Figure 5. High kinetic energy impact. The central crater was apparently blown away by the force of the shock wave



Figure 6. Low velocity impact. The central crater shows no signs of melting; it appears only to be damaged



Figure 7. Extremely oblique impact

Whereas the extended impact features were usually clearly classifiable as such (with some exceptions of contamination looking very similar to them), a variety of "standard" impacts can be found on the germanium surfaces.

Therefore, a further subclassification into four standard impact types was made: (1) Hypervelocity impacts (see figure 4), (2) high kinetic energy impacts (see figure 5), (3) low velocity impacts (see figure 6)

and (4) oblique and highly oblique impacts (see figure 7). This classification is mainly possible with experience gathered from impact features found on surfaces with laboratory produced impacts (see also description of the laboratory experiments below) and by comparison with features documented in the literature (as, for example, [3] and [4]).

Especially the oblique and highly oblique impact features are interesting because the orientation and eccentricity of the central crater can give hints to where the particle may have come from.

HYPERVELOCITY IMPACT EXPERIMENTS IN THE LABORATORY

In order to retrieve information on the impacting particle's properties, it is necessary to perform comparative impact experiments in the laboratory where mass, velocity and chemical composition of the impacting particle can be measured or are known, respectively.

Facility Description

The Lehrstuhl für Raumfahrttechnik operates several high- and hypervelocity impact facilities. The laboratory equipment contains (see also [8]):

- an eddy current accelerator covering low velocities from several cm/s up to 400 m/s for particles up to 100 μm diameter,
- an electrothermal accelerator facility with a velocity range up to 5 km/s for particles with up to 1 mm diameter, and
- a plasmadynamic accelerator for particles in the size range of 5 to 150 μm and velocities up to 20 km/s.

For the laboratory impact experiments we used the plasmadynamic accelerator shown in figure 8.

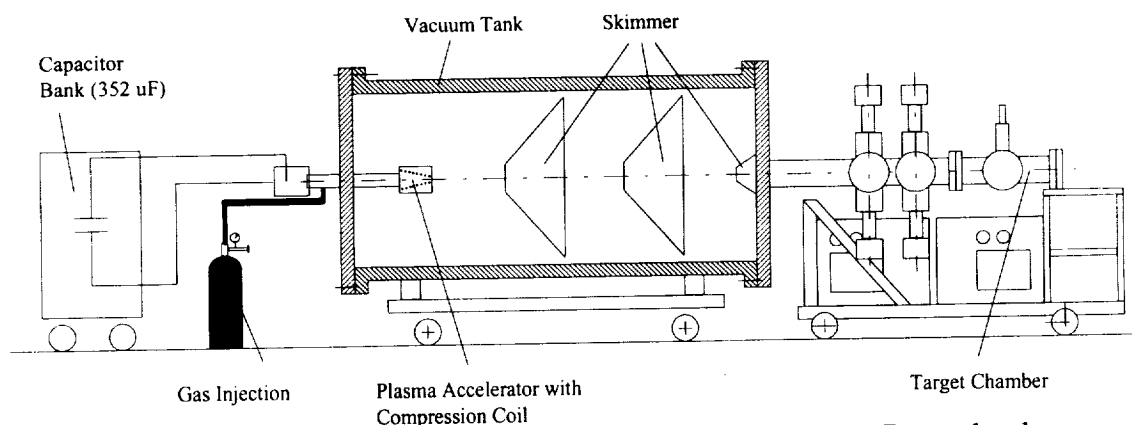


Figure 8. Setup of the plasmadynamic hypervelocity accelerator. Recently, the target chamber has been modified.

The vacuum chambers are evacuated (100 Pa in main chamber, 0.1 Pa in target chamber). To launch particles, the capacitor bank is charged to approximately 16 kV, then Helium is injected into the breech of the coaxial barrel. After triggering, ignitrons switch the discharge, which ionizes the Helium and forms a plasma arc. This plasma is accelerated to about 100 km/s (measured at the barrel muzzle), enters the compressor coil and causes a current to flow from the center electrode to the coil turns. The coil current generates a magnetic field, whose interaction with the currents flowing in the plasma results in Lorentz forces, which in turn compress the plasma. The plasma flow provides a dynamic pressure of up to 1 Billion Pa in the coil muzzle.

The time when the coil is completely filled with plasma is determined via a Rogowsky coil signal. Glass beads placed in the muzzle area are accelerated by the aerodynamic drag. Typical size ranges of these beads are 20-150 μm .

Experiment Evaluation

The particle parameters are measured by detecting the plasma signal from the impact. For this, charge collectors and charge sensitive amplifiers are used as impact detectors mounted close to the surface to be investigated (see figure 9). The impact signal is recorded and can be used for the determination of the time of impact.

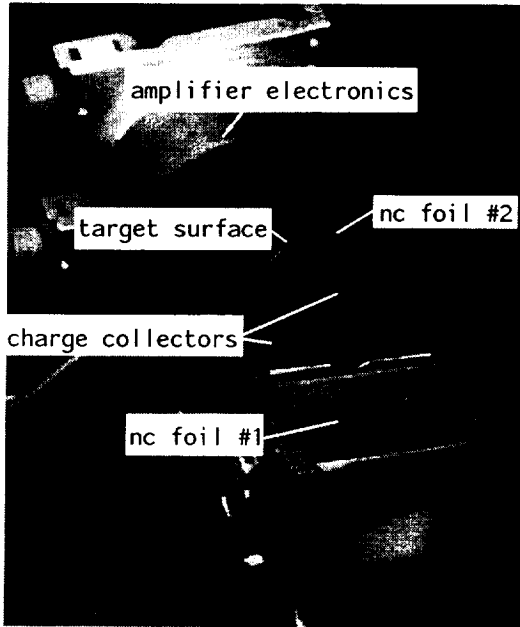


Figure 9. Impact detector used in the Irt plasma accelerator.

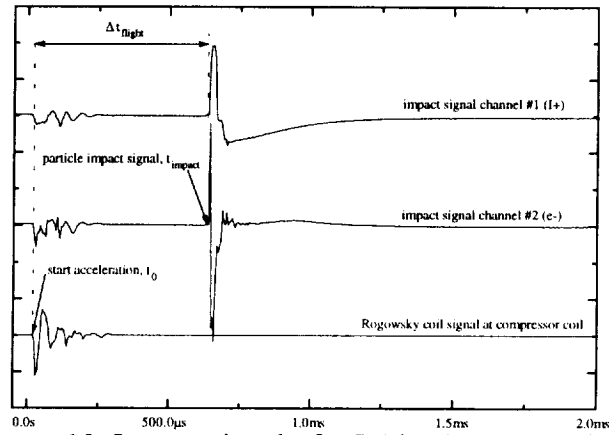


Figure 10. Impact signal of a 7.4 km/s, 54 μm diameter particle

One or two sub micron films in front of the target surface, at a distance of some 100 mm will reveal the particle size since the trace of the particle can be seen after it perforated the foil. Figure 11 shows a penetration hole of one of these particles. In addition, information on ejecta can be gathered, as well, by putting the second foil close to the target, as shown in figure 9.

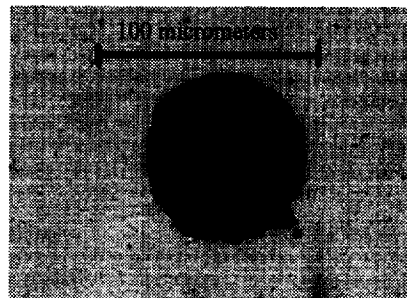


Figure 11. Perforation of witness foil used in the impact detector (revealing a particle diameter 74 μm)

Next, basic crater dimensions are measured using an optical microscope. Both crater diameter and crater depth are measured, the latter by using a differential focusing method. After that, the sample is proc-

essed in the SEM much the same as the LDEF samples to have the geometry of the impact features analyzed. In addition, the laser scanner is used for examination of the impact feature topography.

RESULTS

The following gives an overview on the variety of information that can be retrieved from the LDEF and laboratory experiments.

Feature Analyses of LDEF Surfaces

Crater Size Flux

Figure 12 gives the cumulative average central crater pit diameter flux for the germanium surfaces from E08 for the total exposure time. Note the decrease of the flux numbers for central craters smaller than 4 μm . This might either be due to a decrease in the number of smaller particles at this size regime, or due to our scanning procedure, which was conducted usually at a 100x magnification. Since many of the smaller impacts were located while zooming in on another impact feature, we could have missed some of the smaller craters, as well.

To compensate for this uncertainty, we believe that our data covers *only* those impact features with central crater pits larger than 4 μm . The flux for smaller particles may or may not be higher than these numbers may indicate.

Geometry

Since the aim of our investigations is to deduct particle properties, such as velocity, angle and mass, solely from impact morphology, a look at figure 13 shows an interesting, not yet completely understood relationship. This plot shows the relation between the impact feature's central crater pit area and the total spalled off area for the 615 impact features where the outline has already been redrawn. Since the central crater size is mainly influenced by particle kinetic energy and the spallation mainly by particle velocity, the relationship and the relatively small scatter should be worth having a closer look at.

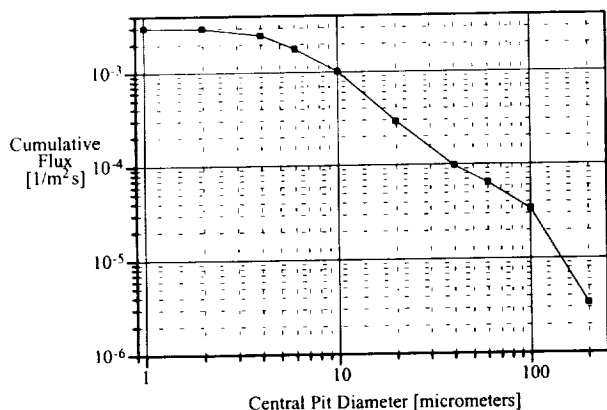


Figure 12. Flux on germanium surfaces in terms of central pit diameter

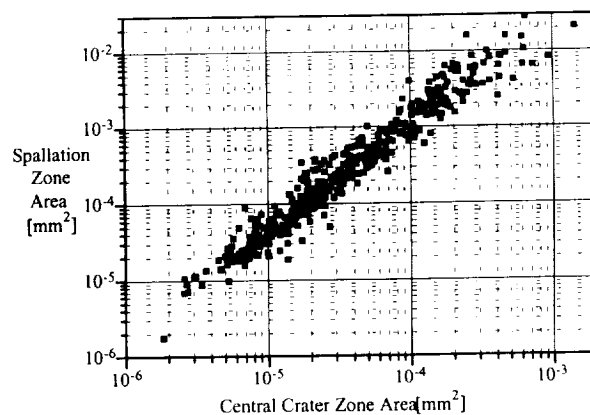


Figure 13. Relationship between central crater and damaged (spalled) area

This relationship has not yet been fully studied. Further experiments in our accelerator facility are currently done to investigate this effect further.

Central Crater Eccentricities

Some of the impact features which were classified as high velocity impacts, i.e. those features that have a molten central crater (see figure 4), show signs of obliquity. Since other LDEF investigators research this field, too, although for different target material, for example [12], we decided to include this phenomenon in our feature evaluation, as well.

We applied a least error squares fit of an ellipse to the central crater outline of those features showing a molten central pit. This resulted in an elliptic curve and revealed directionality information of the impact crater. Figure 13 shows the distribution of the ratio of minor and major axes of the ellipse together with a Gaussian fit on that data. The majority of central craters are almost circular. The small shift toward the 0.9 ratio is consistent with observations made for lunar rocks [7]. There is a reasonable number of impacts with fairly oblique central craters. These might be used for the determination of impact direction.

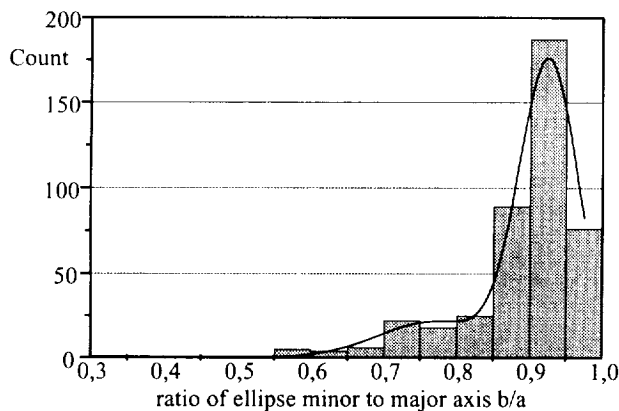


Figure 14. Eccentricity of LDEF central crater fits.

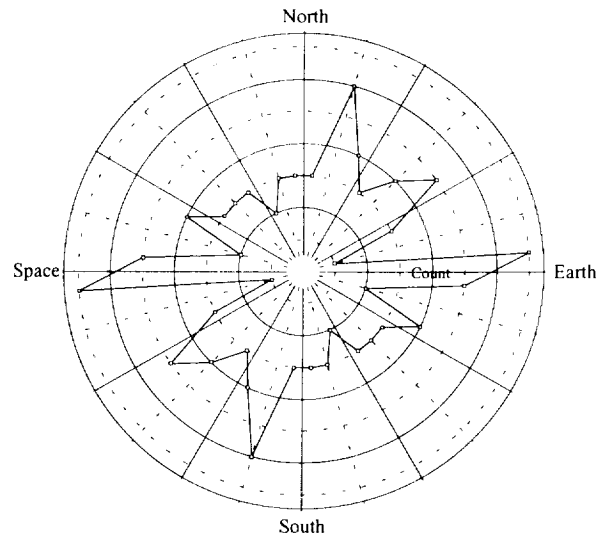


Figure 15. Distribution of direction of major axis ellipse fits for craters with a b/a ratio smaller than 0.7. Coordinate system as if looking from ram direction on bay E08.

Directionality

The direction of the major axis of the impact features with a b/a ratio smaller than 0.7 are plotted in figure 15. Since the direction of the major axis does not tell whether the particle came from one side or the other, this histogram plot is symmetric. There seem to be some preferred impact directions from Space (or Earth), almost North (or South) and Northeast (or Southwest).

Feature Analyses of Laboratory Experiments

The following figures show some of the relationships between particle and impact feature parameters from impact experiments performed in our laboratory.

Particle Size vs. Spallation Zone Size

Figure 16 gives the relationship between particle diameter and damage size (that is, average spallation zone diameter). Note that this data covers the velocity regime from 2 to 17 km/s of laboratory-produced impact features. Since some of the crater forming processes (for example melting of central crater) are

highly velocity-dependent, figure 16 shows an "engineering" relationship for these two parameters, allowing a rough estimate of damage size to germanium surfaces from the common space debris and micrometeoroid flux models by Kessler and Grün or Cour-Palais.

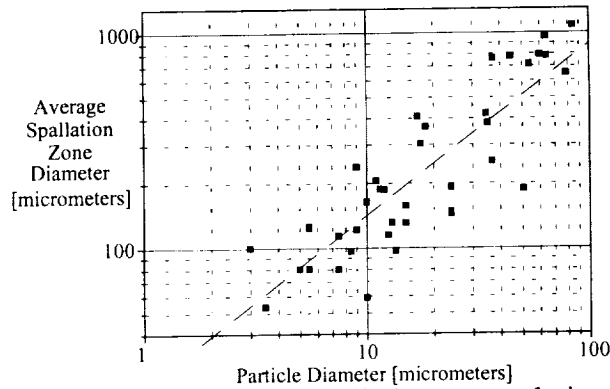


Figure 16. Particle diameter to spallation zone relationship

The parameters for the dotted "engineering" fitting curve are:

$$\log_{10} D_{\text{Spall}} \approx 1.348 + 0.800 \cdot \log_{10} D_{\text{Particle}}$$

(standard deviation 0,19071, n = 39, valid for velocities between 2 and 17 km/s and spherical glass particles)

Eccentricity for Different Impact Angles

Since one of the major issues of our investigations is to get an idea on where the particles came from, it is important to learn more on the influence of the impact angle on crater obliquity. The following impact data was obtained without any velocity or particle size measurement. It resulted in some data points for 0° and 45° impact angle. Unfortunately, for the 70° impact angle experiments, we got only a single impact which is shown in figures 19 through 21.

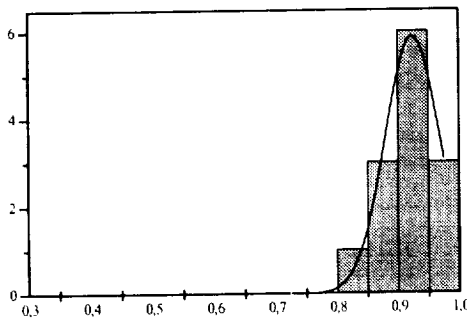


Figure 17. Ratio of major to minor axis of impacts with an impact angle of 0°. (13 impacts)

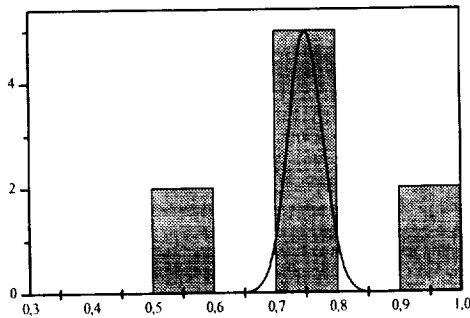
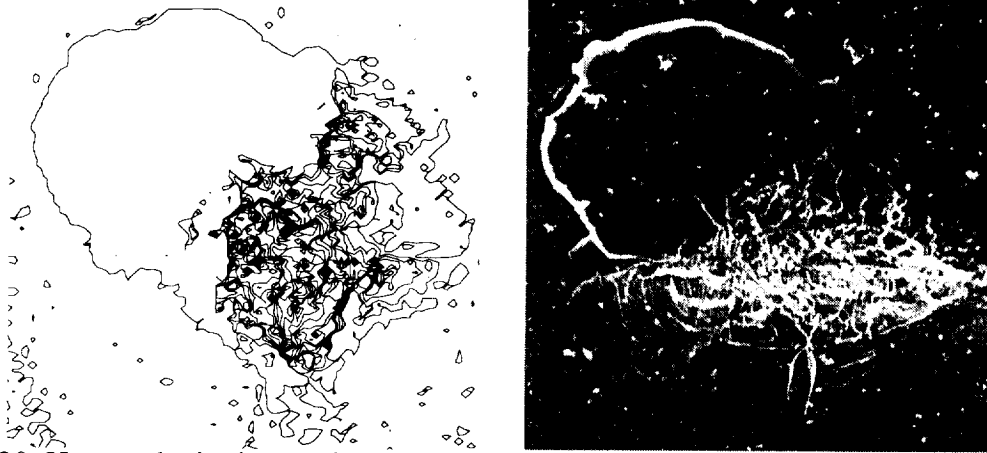


Figure 18. Ratio of major to minor axis of impacts with an impact angle of 45°. (11 impacts)

Figures 17 and 18 give b/a ratio histograms for impacts produced at different angles. Apparently, this ratio shifts to smaller values for increasing impact angles. The effect is not too obvious since the number of data points is not yet significantly high enough for establishing an impact angle-to-crater eccentricity function, but it seems as if central craters in germanium become more oblique at lower impact angles, than for example in aluminum, where usually impact angles larger than roughly 60° are needed for elliptical craters.

Morphology Changes with Impact Angle Variation

As mentioned before, highly oblique impacts show a distinct morphology. Figures 19 through 21 show an impact produced by a particle of unknown speed and size in our plasma accelerator. Impact direction was from the left; particle ejecta is visible at the right side on the SEM image; under the optical microscope the ejecta can be seen to spread over an area almost the same size as the impact feature itself. The feature maps were taken using our 3D laser topographer.



Figures 19 and 20. Hypervelocity impact into germanium at an impact angle of 70° . Velocity and particle size for this particular impact were not measured. Note the ejecta spray on the right side

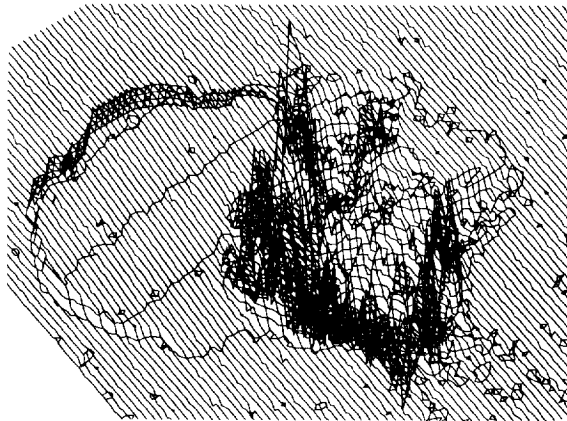


Figure 21. Same impact feature, perspective view.

The angle at which oblique central pits change to this type of feature showing almost ricochet effects has not yet been determined. It seems to be somewhere at 60° or 65° , although mass and velocity effects will have an effect, too.

Combining LDEF and Laboratory Findings

Crater Depth vs. Crater Volume

Since the impact feature morphology for brittle materials is somewhat more complicated than for example aluminum, more parameters can be measured and more effects should have an influence on the shape of the impact feature. Figure 22 shows one of these effects, a plot of the central crater ("penetration") depth vs. the total crater volume (i.e. central crater plus spalled off volume). When plotting the

LDEF data, it appears that there are two distinct clouds of scattered data points visible. Adding the laboratory data this data neighbors the upper cloud of the LDEF data points. The reason for this clustering is not yet understood. It could still be statistical errors, or it could be a density or velocity driven effect, since the glass beads used in our lab resemble space debris as far as density is concerned and the majority of our impact experiments consist of impacts with speeds around 12 km/s.

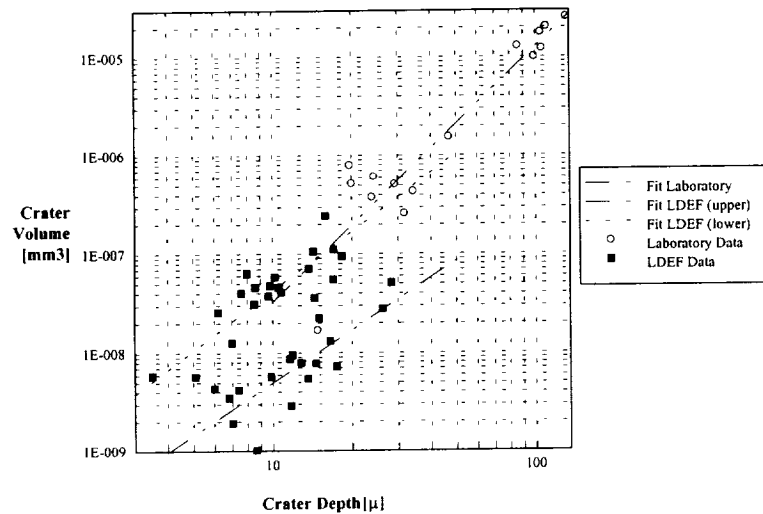
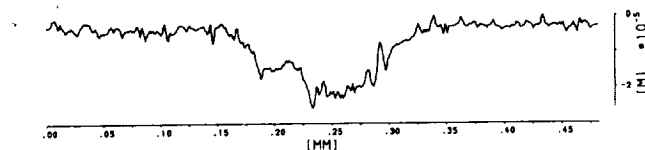


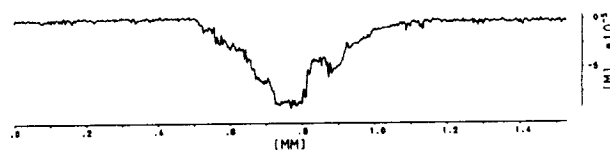
Figure 22. Crater depth vs. total moved volume for LDEF and laboratory impacts.

Cross-Section Changes

As described before, the morphology changes with the impact speeds. Melting occurs at velocities beyond 5-6 km/s. The rims of the central crater become visible in the cross-sections of our laser topographer. Figures 23 through 28 show three craters produced by particles of different velocities. The central crater rim is visible in figure 28 only, which was produced by a hypervelocity particle, as opposed to figure 24 where the central crater region is relatively flat. Also, note the change in the central craters' appearance with an almost circular central crater.



Figures 23 and 24. Image and cross-section of an impact with particle velocity of 2.1 km/s



Figures 25 and 26. Image and cross-section of an impact with particle velocity of 5.6 km/s (High kinetic energy impact due to the size of the particle)

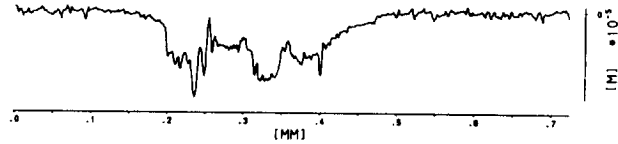
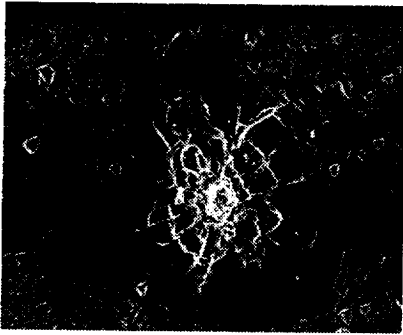


Figure 27 and 28. Image and cross-section of an impact with particle velocity of 7.8 km/s

CONCLUSIONS

Summary of the efforts that have been done so far:

- Crater morphology analysis should be able to provide information on certain particle parameters, such as velocity and kinetic energy, and, at least for some impacts, direction.
- This may not be possible for individual craters but rather for a large number of impact features.

We will have to continue our work; it is especially necessary to:

- collect more cross-sectional data of LDEF impact features.
- Together with impact data for other materials, such as aluminum, which was collected at our facility before, more calibration data for different surface materials should become available in near future.
- Analysis of ejecta, in that case, large chips, produced during the impact could give more information on brittle surface materials as sources of orbital debris particles.
- Also, we will continue our efforts to put a Mosaic server on-line. Currently, an experimental database is available via INTERNET connection to

asterix.lrt.mw.tu-muenchen.de [129.187.218.2]

NOTE

This work was supported by DARA (Deutsche Agentur für Raumfahrtangelegenheiten) GmbH contract 50 QV 9194 0. The author is responsible for the content of this paper.

LITERATURE

1. Allbrooks, M. Atkinson, D., *The Magnitude of Impact Damage on LDEF Materials*, NASA Contractor Report NCR 188258, NASA JSC and Lockheed ESC, 1993
2. Amari, S., Foote, J., Simon, C., Swan, P., Walker, R.M., Zinner, E., Jessberger, E.K., Lange, G., Stadermann, F., *SIMS Chemical Analysis of Extended Impact Features from the Trailing Edge Portion of Experiment A0187-2*, in: *Proceedings 1st LDEF Post-Retrieval Conference*, NASA CP-3134, 1992

3. Brownlee, D., Bucher, W., *Primary and Secondary Micrometeoroid Impact Rate on the Lunar Surface: A Direct Measurement*, in: *Analysis of Surveyor 3 material and photographs returned by Apollo 12*, NASA SP-28, 1972
4. Cour-Palais, B.G., *Hypervelocity Impacts in Metals, Glass and Composites*, *Int. J. Impact Engineering*, Vol. 5, pp. 221-237, 1987
5. Fechtig, H., Gentner, W., Hartung, J.B., Nagel, K., Neukum, G., Schneider, E. Storzer, D., *Microcraters on Lunar Samples*, *The Soviet-American Conference On Cosmochemistry Of The Moon And Planets*, NASA SP-370, 1977
6. Flaherty, R. E., *Impact Characteristics in Fused Silica for Various Projectile Velocities*, *Journal of Spacecraft*, Vol. 7, No. 3, pp. 319-324, 1970
7. Hörz, F., Morrison, D.A., Gault, D.E., Oberbeck, V.R., Quaide, W.L., Vedder, J.F., Brownlee, D.E., Hartung, J.B., *The Micrometeoroid Complex and Evolution of the Lunar Regolith*, *The Soviet-American Conference On Cosmochemistry Of The Moon And Planets*, NASA SP-370, 1977
8. Igenbergs, E. et al, *Launcher Technology, In-Flight Velocity Measurement and Impact Diagnostics at the TUM/LRT*, *International Journal of Impact Engineering*, Vol. 5, pp. 371-380, 1987
9. Iglseider, H., Igenbergs, E., *Measured Charge Generation By Small Mass Impact At Velocities Between 1 and 45 km/s*, *International Journal of Impact Engineering*, Vol. 5, pp 381-388, 1987
10. Kemp, W.T. et. al, *Long Duration Exposure Facility Space Optics Handbook, Final Report*, Phillips Laboratory, Kirtland AFB, PL-TN--93-1067, 1993
11. Kreitmayer, U., *Konstruktion und Bau eines Teilchendetektors für das Raumfahrtexperiment LDEF*, *Diplomarbeit (Master's Thesis)*, Lehrstuhl für Raumfahrttechnik, RT-DA 82/3, 1982
12. Mackay N.G. et al, *Interpretation Of Impact Crater Morphology And Residues On LDEF Using 3D Space Debris And Micrometeoroid Models*, *Proc. First European Conference On Space Debris*, ESA SD-01, 1993
13. Mandeville, J.-C., *Profile and Depth of Microcraters formed in Glass*, *Earth and Planetary Science Letters* 15 (1972) 110-112, 1972
14. Vedder, J. F., *Microcraters Formed in Glass by Projectiles of Various Densities*, *Journal of Geophysical Research*, Vol. 79, No. 23, 1974

* Currently at North Carolina State University, College of Engineering, Analytical Instrumentation Facility, Box 7916, Raleigh, NC 27695-7916